

03 Jun 1993, 2:00 pm - 4:00 pm

Gravelly Soil Properties by Field and Laboratory Tests

Takaaki Konno

Kajima Corporation, Tokyo, Japan

Yoshio Suzuki

Takenaka Corporation, Tokyo, Japan

Akira Tateishi

Taisei Corporation, Tokyo, Japan

Kenji Ishihara

University of Tokyo, Tokyo, Japan

Kinji Akino

Nuclear Power Engineering Corporation, Tokyo, Japan

See next page for additional authors <https://scholarsmine.mst.edu/icchge>



Part of the [Geotechnical Engineering Commons](#)

Recommended Citation

Konno, Takaaki; Suzuki, Yoshio; Tateishi, Akira; Ishihara, Kenji; Akino, Kinji; and Iizuka, Setsuo, "Gravelly Soil Properties by Field and Laboratory Tests" (1993). *International Conference on Case Histories in Geotechnical Engineering*. 9.

<https://scholarsmine.mst.edu/icchge/3icchge/3icchge-session03/9>

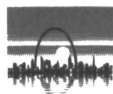


This work is licensed under a [Creative Commons Attribution-Noncommercial-No Derivative Works 4.0 License](#).

This Article - Conference proceedings is brought to you for free and open access by Scholars' Mine. It has been accepted for inclusion in International Conference on Case Histories in Geotechnical Engineering by an authorized administrator of Scholars' Mine. This work is protected by U. S. Copyright Law. Unauthorized use including reproduction for redistribution requires the permission of the copyright holder. For more information, please contact scholarsmine@mst.edu.

Author

Takaaki Konno, Yoshio Suzuki, Akira Tateishi, Kenji Ishihara, Kinji Akino, and Setsuo Iizuka



Gravelly Soil Properties by Field and Laboratory Tests

Takaaki Konno
Kajima Corporation, Tokyo, Japan

Yoshio Suzuki
Takenaka Corporation, Tokyo, Japan

Akira Tateishi
Taisei Corporation, Tokyo, Japan

Kenji Ishihara
University of Tokyo, Tokyo, Japan

Kinji Akino and Setsuo Iizuka
Nuclear Power Engineering Corporation, Tokyo, Japan

SYNOPSIS: The basic policy in Japan is to build nuclear reactor buildings on rock. But, in order to cope with the middle and long term siting problems it has become necessary to develop new siting technology from the standpoint of expanding the available range of site selections and effective utilization of lands. The gravelly soil layer in the Quaternary deposits has high possibility of becoming the bearing soil stratum when constructing a nuclear power plant. In order to verify the seismic stability of such gravelly soil layers, a series of field dynamic and static torsional loading tests for large scale in-situ soil columns were performed. In addition, a series of laboratory tests using a large scale triaxial test apparatus on high quality undisturbed gravel samples obtained by in-situ freezing method were performed. Herein reported are the sampling method of high quality undisturbed samples, laboratory test results and the large in-situ soil column test results.

INTRODUCTION

The investigation of the siting technology reported herein is an entrusted project to Nuclear Power Engineering Corporation (NUPEC) from Ministry of International Trade and Industry of Japan (MITI), and has been executed under the cooperation of academic and industrial groups. The planning on verification of soil seismic stability was commenced in 1983, and large scale field tests were implemented from 1987 to 1988 at the Tadotsu Engineering Laboratory, Kagawa Prefecture, Japan, of NUPEC. For the field testing, two soil columns with 10m in diameter but with different depths of 5m and 9m, a concrete block weighing 30MN with earth contact pressure of 470 kPa which is equivalent of actual reactor building, and a reaction block weighing approximately 50MN were built, and the verification test of soil seismic stability was executed by dynamic and static loading tests. (See Fig. 1 and Fig. 2). Moreover, to supplement the field conditions, laboratory tests simulating the seismic input were performed using scaled-down models. The objectives of this paper are to present the soil profile of the test site, sampling method, laboratory test results

on high-quality undisturbed samples of gravelly soils, test results of large in-situ soil columns and the soil properties obtained from comparison of both test results which were performed in 1985 to 1989.

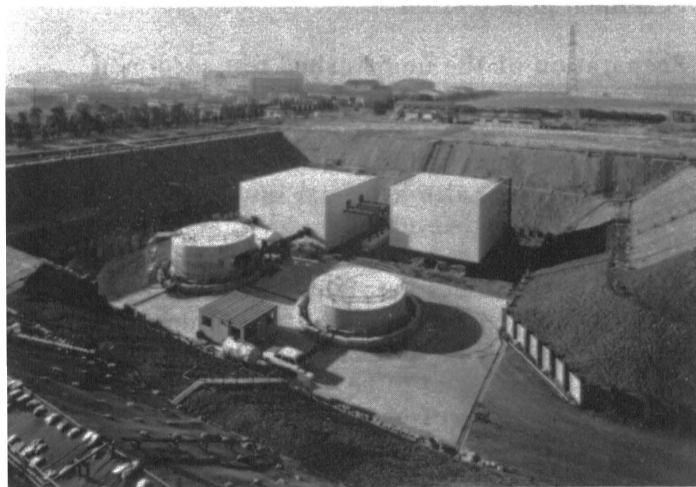


Fig. 1 General view of the field test model

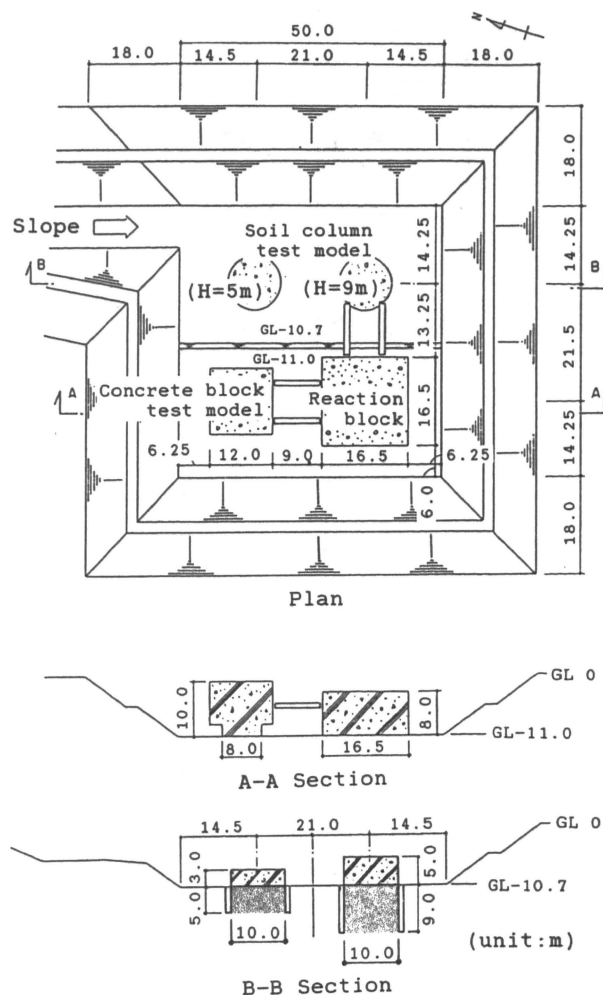


Fig. 2 Layout of the field test model

SOIL PROFILE OF THE TEST SITE

Shown in Fig. 3 are typical soil layer composition of the test site, penetration resistance value (N and NL) of the standard penetration test (SPT) and the large scale penetration test (LPT), and the distribution of the shear wave velocity (V_s) through the depth obtained by the down-hole method. The test site is composed of reclaimed soil of dredged material 11 m in thickness from the surface, underlaid by a diluvial gravelly soil layer from the depth of 11m to 20m. This gravelly soil layer has a shear wave velocity (V_s) of 380m/sec with N values of 40 to 50. The value of NL in this gravelly layer is between 15 and 40.

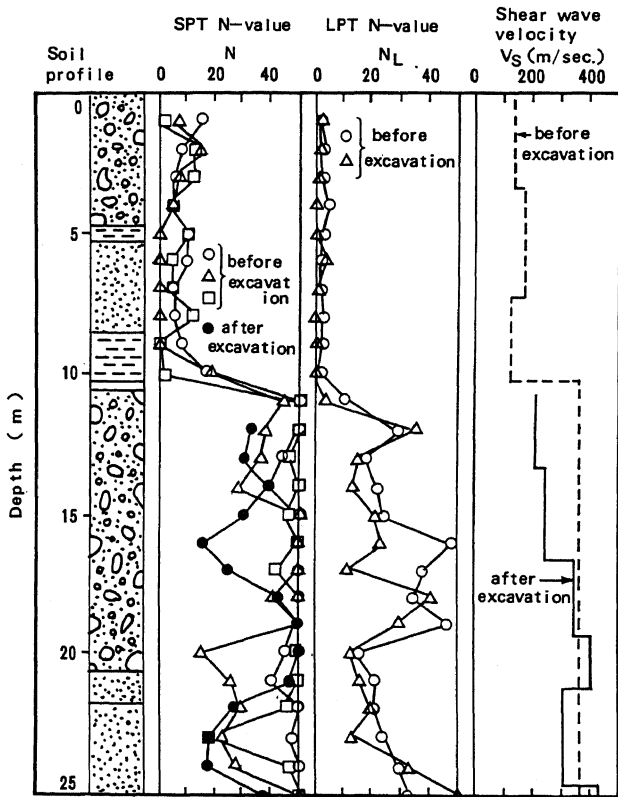


Fig.3 Soil profile of test site

METHOD FOR OBTAINING HIGH-QUALITY UNDISTURBED GRAVEL SAMPLES

It is well known that soil properties obtained by laboratory tests are influenced largely by sampling method (Yoshimi et al, 1984 ; Hatanaka et al, 1985, Hatanaka et al, 1988). The in-situ freezing sampling method which is considered the best in the present state-of-the-art technique therefore was adopted to recover high-quality undisturbed samples from gravelly deposit.

Installation of freezing pipes

A 140 cm hole was drilled down to a depth of 12.7 m using the earth drilling machine. Five guide pipes fixed by two steel plates at both ends were installed into the bottom of the 140cm hole in order to exactly determine the locations of the freezing pipe and sampling places (Fig. 4(a)).

With the guidance of the 164 mm steel pipe, a hole of about 76 mm in diameter was drilled down to a depth of about 20 meter. A steel tube 73mm in diameter was installed into the 76mm hole down to a depth of about 20 m.

A stainless steel pipe 21.7mm in diameter was placed in the 73 mm steel tube.

The liquid nitrogen supplied from the upper end of the stainless steel pipe flows down to the bottom of the pipe and rises in the annular space between the two freezing pipes (Fig. 4(b)).

Ground freezing and undisturbed sampling

Liquid nitrogen was supplied from a lorry for about 160 hours to freeze the soil around the 73mm steel tube to a diameter of about 140cm as shown in Fig. 4(c). Sampling of frozen soil from the undisturbed area was done by lowering the double-tube core barrel by rotating it with a boring machine using chilled mud (Fig. 4(d)). The frozen sample has been cored in the inner tube and pulled up using a center-hole jack (Fig. 5). The tensile load required to cut the frozen sample from the ground ranges 6 to 13 tons. It took about 16 to 35 minutes for lowering the core tube about 100cm in depth. Fig. 6 shows the frozen sample cored by the double-tube core barrel.

Specimen preparation

Preparation of the undisturbed test specimen was performed in the field. After the frozen sample was pulled out from the inner tube of the double-tube core barrel, it was cut to a length of 60cm with a special saw (Fig. 7). Fig. 8 shows a close-up of the cylindrical surface of the prepared specimen. The perfect smoothness of the surfaces cut, minimizes the effects of membrane penetration during undrained tests. In the previous studies, this effect has been considered to be significant for reconstituted specimens of gravelly soil.

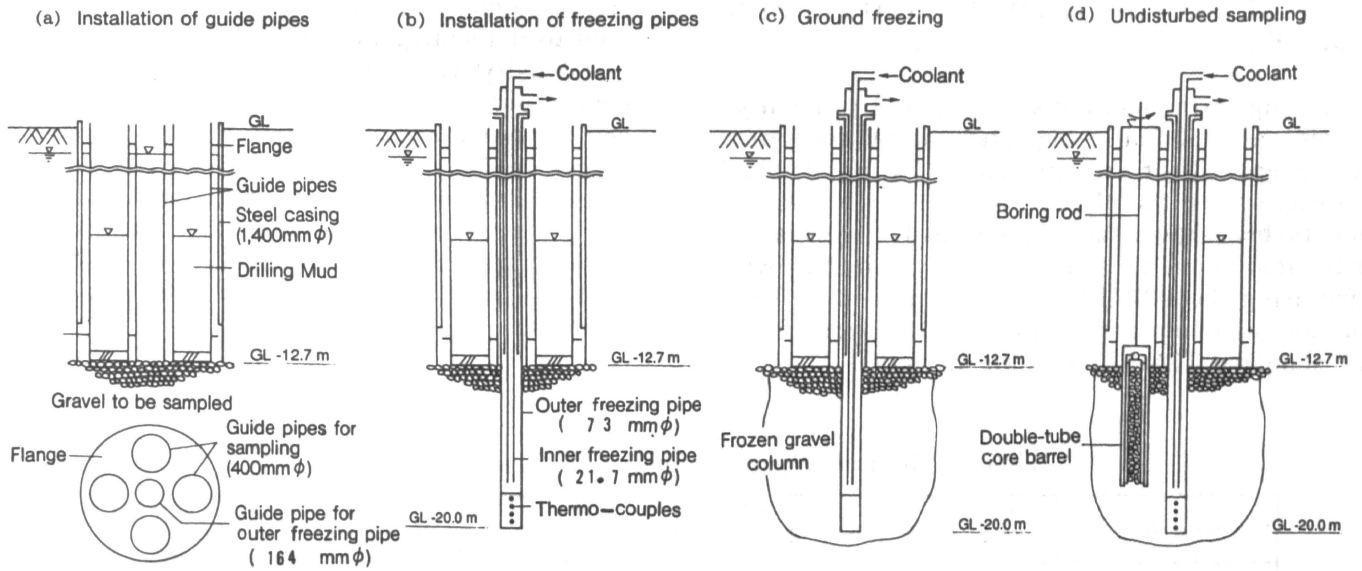


Fig.4 Procedure of in-situ freezing sampling

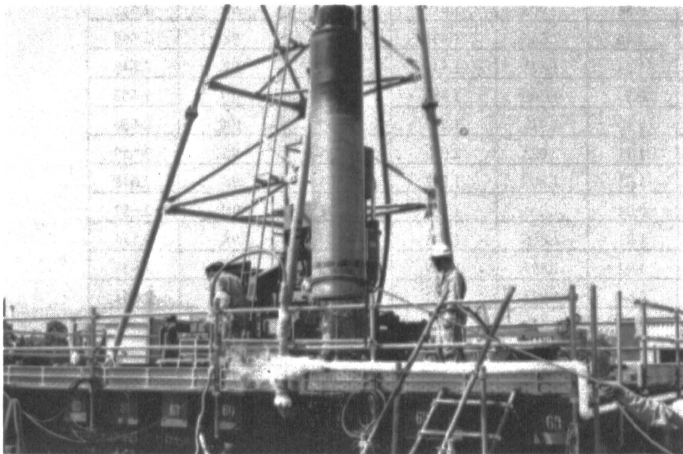


Fig.5 Double tube core barrel being lifted up from the ground



Fig.6 Frozen gravel sample from a core-barrel

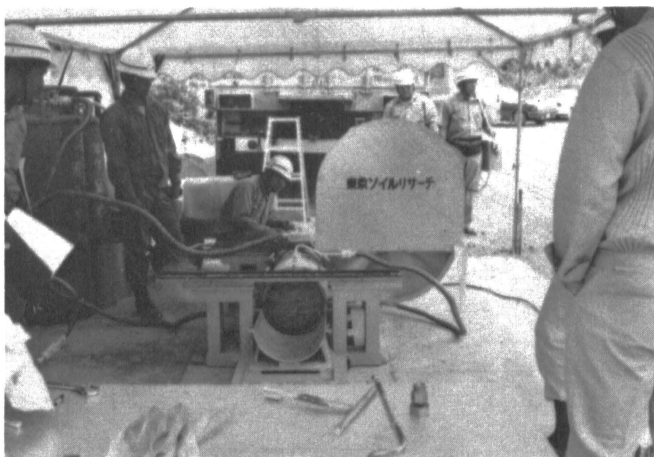


Fig.7 A special diamond saw

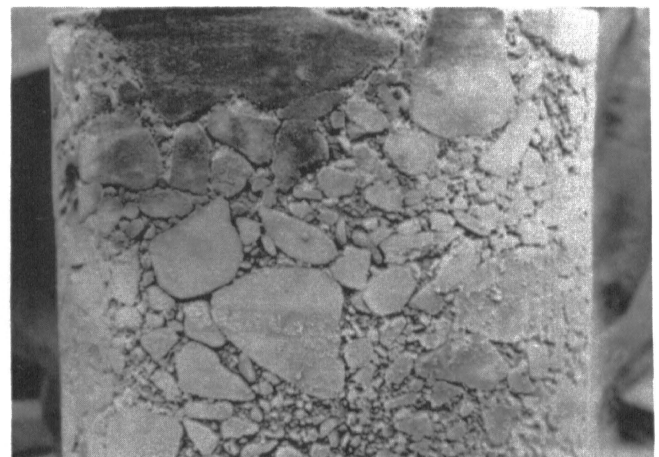


Fig.8 A close-up of the sample surface

PHYSICAL PROPERTIES OF IN-SITU FROZEN SAMPLES

According to the method shown in Fig.4, twenty samples each 30 cm in diameter and 60 cm long, were prepared for the laboratory testing. Table 1 and Fig.9 show the physical properties of the undisturbed gravel samples tested. Determination of the maximum and minimum dry densities was done using the JSSMFE Standard Method of Test for the Maximum and Minimum Densities of sand, JSF standard T26-81T (JSSMFE, 1979). A steel

mold, 30 cm in diameter and 30 cm in depth, was used to determine the limiting densities. Minimum dry density was achieved by placing gravel very gently and slowly into the mold. Maximum dry density was made as follows. The gravels were placed in 7 layers into the mold. After each layer of gravels had placed, the steel mold was vibrated using a small vibrator. After the last layer had been compacted, the top surface was made flat by packing small soil particles between gravel components.

Table 1 Physical properties of undisturbed gravel specimen tested

| Kind of test | Sampling depth GL-(m) | 10% diameter (mm) | 50% diameter (mm) | Maximum diameter (mm) | Uniformity coefficient | Fines content (%) | Dry density γ_d (g/cm ³) | Maximum dry density γ_{dmax} (g/cm ³) | Minimum dry density γ_{dmin} (g/cm ³) | Relative density D_r (%) | Specific gravity G_s | |
|--|-----------------------|-------------------|-------------------|-----------------------|------------------------|-------------------|---|--|--|----------------------------|------------------------|-------|
| ① Undrained cyclic strength test | 1 | 17.70 | 0.91 | 9.2 | 100 | 14.2 | 0.60 | 1.952 | 1.959 | 1.708 | 97 | 2.644 |
| | 2 | 17.80 | 0.76 | 10.5 | 150 | 20.8 | 0.62 | 1.927 | 1.977 | 1.667 | 86 | 2.644 |
| | 3 | 18.00 | 0.47 | 6.0 | 85 | 19.8 | 0.43 | 1.866 | 1.887 | 1.952 | 93 | 2.644 |
| | 4 | 18.25 | 0.72 | 10.0 | 150 | 20.9 | 0.59 | 1.822 | 1.833 | 1.648 | 94 | 2.644 |
| ② Cyclic deformation test | 1 | 14.90 | 0.39 | 12.0 | 115 | 43.6 | 0.58 | 1.908 | 1.912 | 1.658 | 98 | 2.648 |
| | 2 | 14.90 | 1.05 | 17.1 | 110 | 21.7 | 0.46 | 1.945 | 1.951 | 1.682 | 98 | 2.648 |
| | 3 | 15.35 | 0.36 | 2.9 | 85 | 21.7 | 1.34 | 1.824 | 1.841 | 1.640 | 92 | 2.648 |
| | 4 | 15.95 | 0.67 | 7.0 | 105 | 14.9 | 0.27 | 1.860 | 1.857 | 1.662 | 101 | 2.652 |
| | 5 | 18.95 | 0.60 | 11.5 | 105 | 25.3 | 0.80 | 1.919 | 1.892 | 1.655 | 109 | 2.650 |
| | 6 | 19.30 | 0.44 | 12.8 | 110 | 39.3 | 1.11 | 2.023 | 2.037 | 1.715 | 96 | 2.650 |
| ③ Static drained strength test | 1 | 15.55 | 0.42 | 5.5 | 95 | 22.9 | 1.31 | 1.809 | 1.812 | 1.555 | 98 | 2.648 |
| | 2 | 16.30 | 0.85 | 8.9 | 95 | 15.1 | 0.74 | 1.904 | 1.898 | 1.591 | 101 | 2.652 |
| | 3 | 16.80 | 0.40 | 11.9 | 70 | 41.8 | 1.91 | 1.866 | 1.871 | 1.600 | 98 | 2.654 |
| | 4 | 16.90 | 0.46 | 13.0 | 115 | 38.0 | 1.92 | 1.899 | 1.899 | 1.593 | 100 | 2.654 |
| | 5 | 17.05 | 0.29 | 8.5 | 100 | 50.0 | 2.64 | 1.923 | 1.872 | 1.574 | 114 | 2.654 |
| | 6 | 17.30 | 0.28 | 9.4 | 85 | 56.4 | 2.61 | 1.887 | 1.891 | 1.582 | 98 | 2.654 |
| ④ Isotropic compression and expansion test | 1 | 15.85 | 0.93 | 9.5 | 70 | 14.0 | 0.56 | 1.870 | 1.865 | 1.563 | 101 | 2.652 |
| | 2 | 16.25 | 1.09 | 13.9 | 75 | 17.3 | 0.41 | 1.927 | 1.922 | 1.671 | 101 | 2.652 |
| ⑤ Cyclic volumetric strain test | 1 | 14.90 | 1.05 | 17.1 | 110 | 21.7 | 0.46 | 1.945 | 1.951 | 1.682 | 98 | 2.648 |
| | 2 | 15.35 | 0.36 | 2.9 | 85 | 21.7 | 1.34 | 1.824 | 1.841 | 1.640 | 92 | 2.648 |

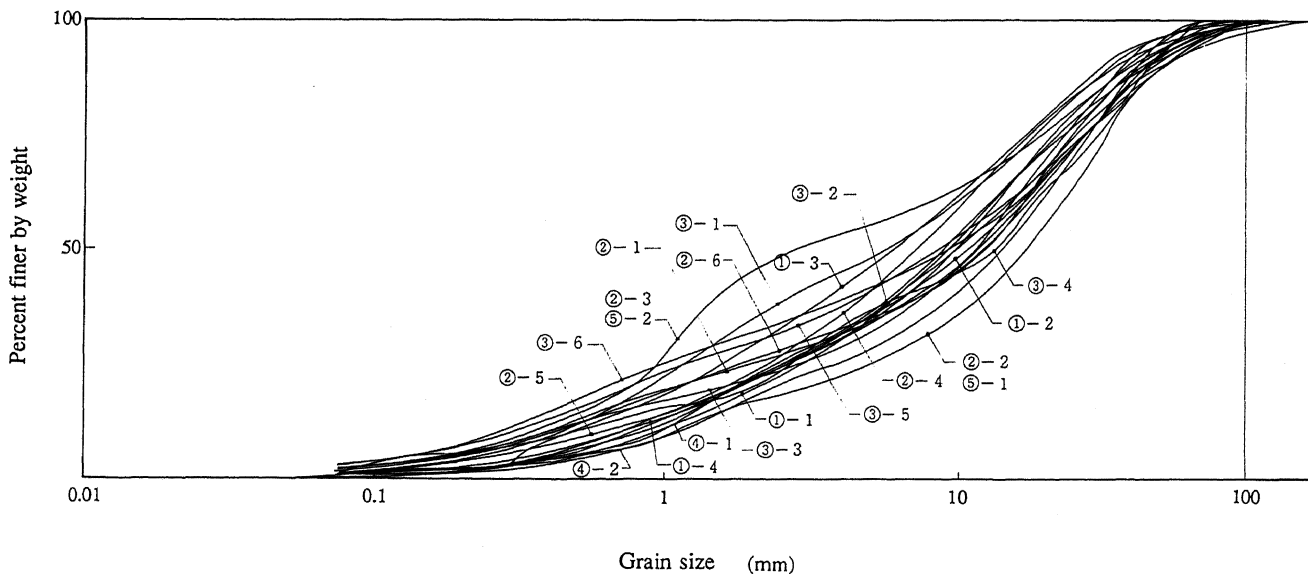


Fig.9 Grain size distribution of gravel samples tested

LABORATORY TESTS ON IN-SITU FROZEN SAMPLES

Test apparatus and test method

Five different types of laboratory tests were performed on undisturbed gravel samples using a large scale triaxial test apparatus shown in Fig.10.

The specific laboratory test methods were; (1) undrained cyclic strength test (liquefaction test), (2) cyclic deformation test, (3) consolidated drained triaxial compression test, (4) isotropic compression and expansion test and, (5) test for obtaining volume change characteristics during cyclic shear.

The confining stress was applied pneumatically and the cyclic axial load applied by hydraulic pressure. The load cell and non contact type displacement sensors were placed inside the cell to determine the stress-strain relationship reliably at low strain levels. The displacement transducer (LVDT) was installed outside the cell for measuring large strain in test method (1) and (3). The volume change during isotropic compression and expansion test was measured by differential pressure transducer.

All the cyclic tests were conducted by applying uniform sinusoidal cycles of deviator stresses at a frequency of 0.01 Hz. The low frequency was selected in order to maintain the constant deviator stress amplitude and also for measuring the axial and volumetric strain accurately.

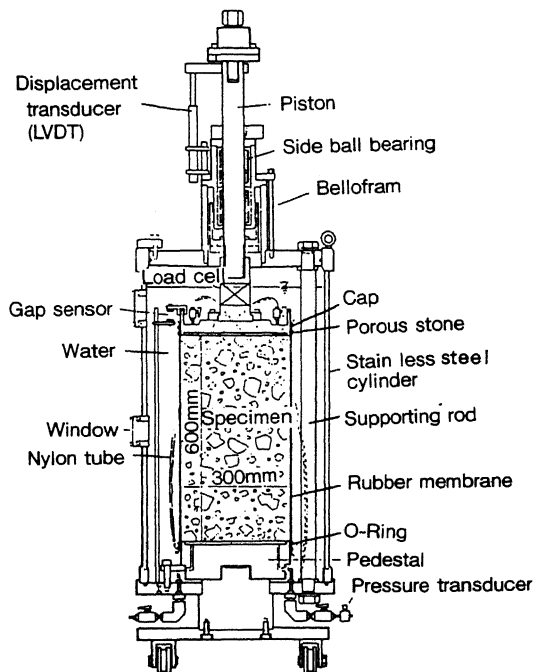


Fig.10 Large scale triaxial test apparatus

LABORATORY TEST RESULTS

Undrained cyclic strength

The test results on both undisturbed and reconstituted samples obtained by undrained cyclic triaxial tests are shown in Fig.11 where it can be seen that the undisturbed samples show a high value of cyclic shear stress ratio of 0.44 required to cause a double-amplitude axial strain of 2.5% in 20 cycles of load application. The strength of reconstituted samples is only about one half that of the undisturbed samples, and the strength of the in-situ gravelly soil would be underestimated if the reconstituted soils are used for the tests.

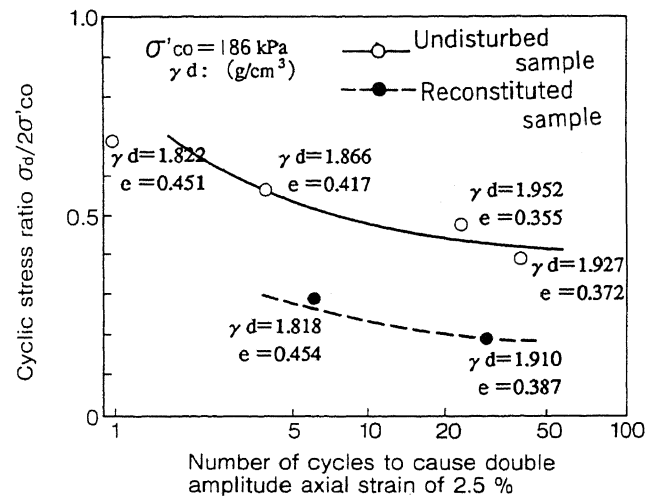


Fig.11 Undrained cyclic shear strength

Fig.12 shows typical stress-strain relationships of the undisturbed specimen under the cyclic stress application. The stress strain relationships show the so-called reverse-S curves which resemble the stress-strain relationship observed for undisturbed dense sand as reported by Yoshimi et al. (1984). We can also clearly see that axial strain progresses significantly on the extension side. Fig.13 shows a stress path of the undisturbed gravel sample during the undrained cyclic shear.

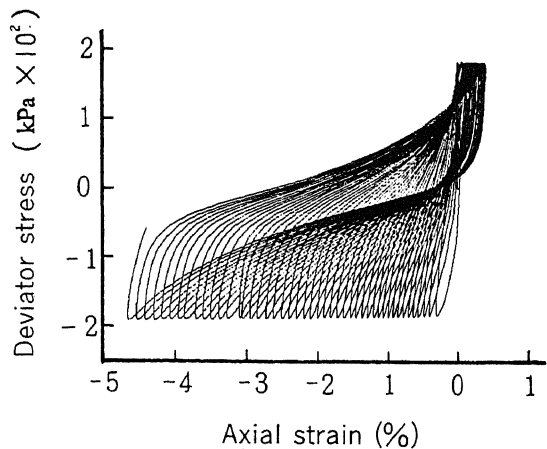


Fig.12 Stress-strain relationship under cyclic undrained shear

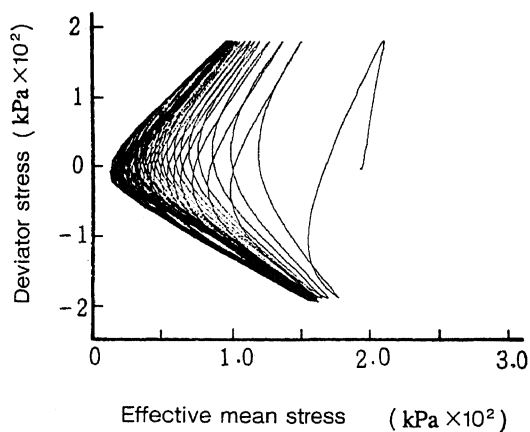


Fig.13 Stress path under undrained cyclic shear

Cyclic deformation characteristics

Test results obtained by cyclic undrained triaxial tests are shown in Fig.14. For comparison, the results of reconstituted samples are also shown. The shear modulus, G , obtained by reconstituted samples are only about one half of that of the undisturbed samples, and as in the case with strength evaluation, it indicates that the deformation characteristics of the in-situ gravelly soil cannot be evaluated by means of tests on reconstituted samples.

Fig.15 shows the $G/G_0 \sim \gamma$ relation for both undisturbed and reconstituted samples. G_0 is the G at the strain level of about 10^{-5} . Unlike the big difference of $G \sim \gamma$ and $h \sim \gamma$ relation between undisturbed and reconstituted samples, there is only little difference of $G/G_0 \sim \gamma$ relation between undisturbed sample and reconstituted sample.

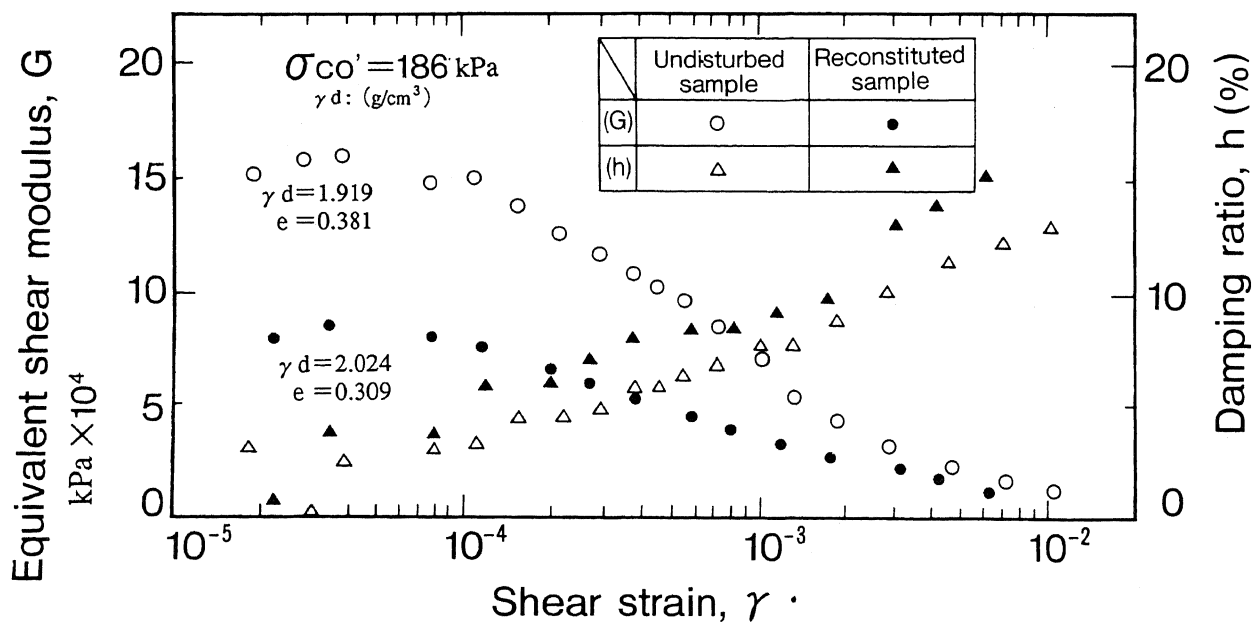


Fig.14 $G_{eq} \sim \gamma$, $h \sim \gamma$ relationships

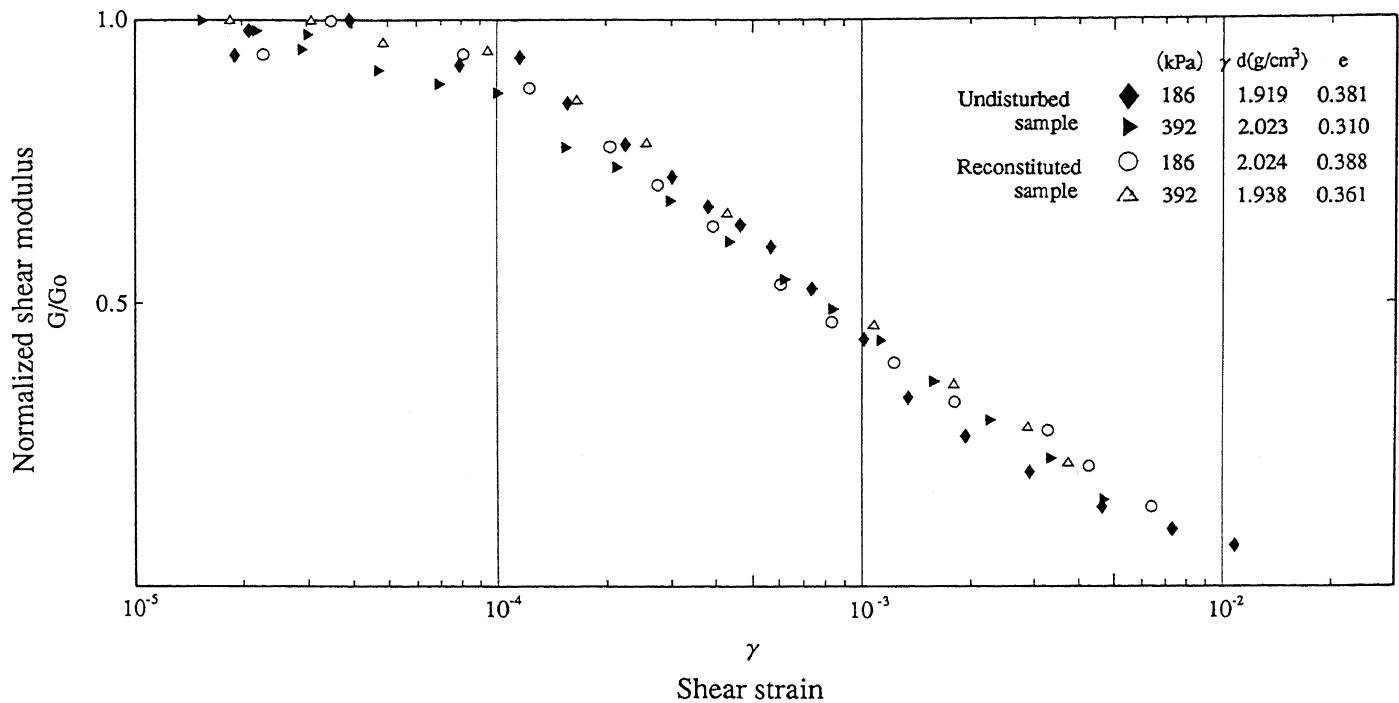


Fig.15 $G/Go \sim \gamma$ relationships for undisturbed and reconstituted samples

Fig.16 shows the relation of the Go and the confining stress, on both logarithmic coordinates. An approximate straight line relation is observed. The slope of this straight line is about 0.8, which is larger than the value of 0.5 commonly known for sand. This fact means that in the gravelly soils, effects of confining stress upon the shear modulus is more significant than that for the sand.

Also shown in Fig.16 is the Go of reconstituted samples with $\sigma' c'$, it can be seen that there is also a straight line relation between Go and $\sigma' c'$ on log-log coordinates. And the inclination of the line is almost same as that of the undisturbed samples of nearly 0.8. This fact means that higher dependency of Go on $\sigma' c'$ does not depend on the sample disturbance.

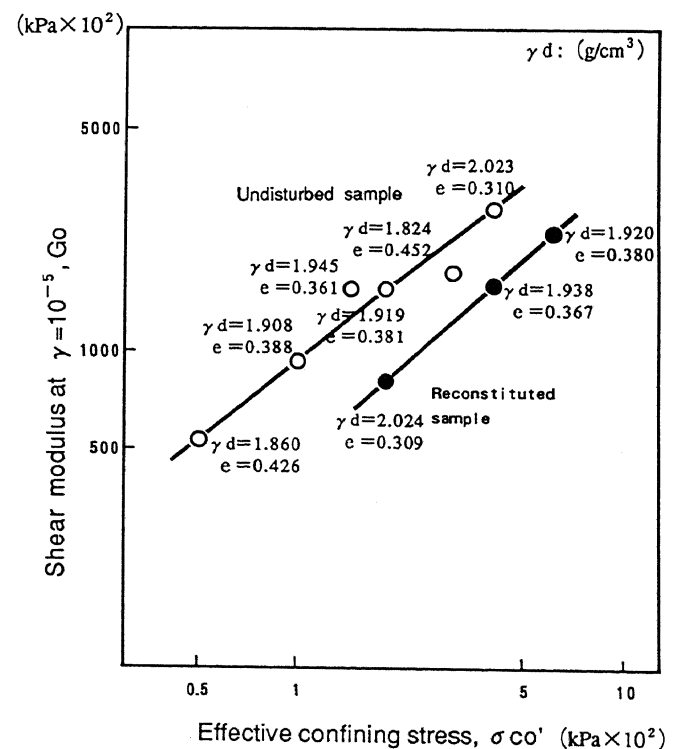


Fig.16 Relationships between Go and $\sigma' c'$

Static strength characteristics

The Mohr's circles at failure obtained by consolidated drained triaxial compression tests are shown in Fig.17. The internal friction angle of the undisturbed specimen is 36 to 37 degree, and the cohesion is 24.5 to 66.6 kPa. The internal friction angle, $\phi' d'$, estimated from N value (on the average, N=43) using the empirical formula equation(1), which is proposed by Dunham for design purposes, is 48 degree. There is a significant difference between the estimated and the measured $\phi' d'$ value on the undisturbed samples. However, there is some cohesion component that may be considered in the actual design works.

$$\phi' d' = \sqrt{12N} + 25 \quad (1)$$

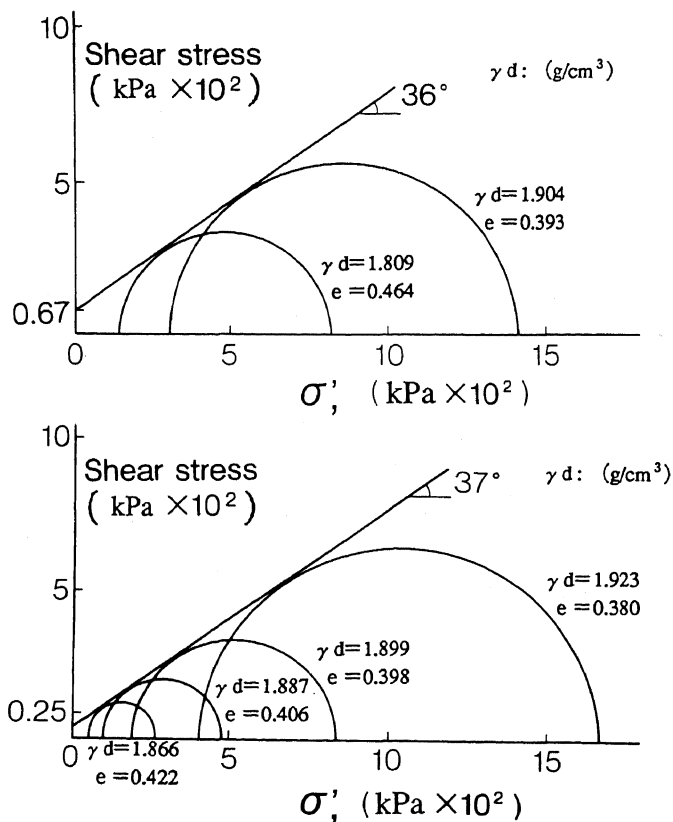


Fig.17 Mohr's circle and failure envelope

Isotropic compression and expansion characteristics

The coefficient of volume compressibility and the coefficient of volume expansion were also measured using a large scale triaxial test apparatus on undisturbed samples as follows:

- (1) After the undisturbed sample had been thawed and saturated, it was stressed isotropically under an initial effective stress of 19.6kPa.
- (2) After that the isotropical stress was increased to a certain level, and then unloading was executed back to the initial isotropical stress of 19.6kPa.
- (3) And then the isotropical stress was increased to a certain value which is larger than that applied in the former loading step.

Fig.18 shows an example of relationship between the isotropical stress and the induced volumetric strain. From the Fig.18, the coefficient of the volume compressibility is estimated to have a value ranging from 1.4×10^{-3} to $6.7 \times 10^{-3} \text{ kPa}^{-1}$, and the coefficient of volume expansion between 2.1×10^{-3} and $5.7 \times 10^{-3} \text{ kPa}^{-1}$.

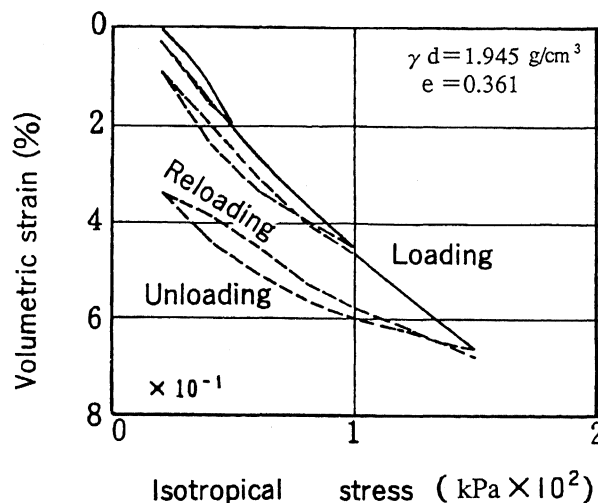


Fig.18 e-logp relationship under isotropical compression and expansion

TORSIONAL TESTS ON LARGE IN-SITU SOIL COLUMNS

In-situ soil columns

In order to expose the diluvial gravelly deposit, the reclaimed soil was excavated, and from this exposed surface two soil columns were cut out by digging annular-shaped trenches of 10m in inner diameter, 80cm wide, and 9m and 5m deep respectively in the gravelly soil layer. The underground water level was maintained below 1.5m from the exposed surface. The side-face of the trench wall was protected by placing mudwater mortar, and rubber bags were lowered into the annular-shaped trench and inflated with water in order to support the inside soil columns laterally as shown in Fig.19.

Then, capping concrete blocks were mounted on top of the soil columns in order to facilitate transfer of cyclic load from loading devices. The confining pressure existent prior to excavation was applied to the soil columns by the weight of the capping concrete block and through the water pressure in the rubber bag. The outline of the in-situ soil columns is shown in Fig.19. and Fig.20.

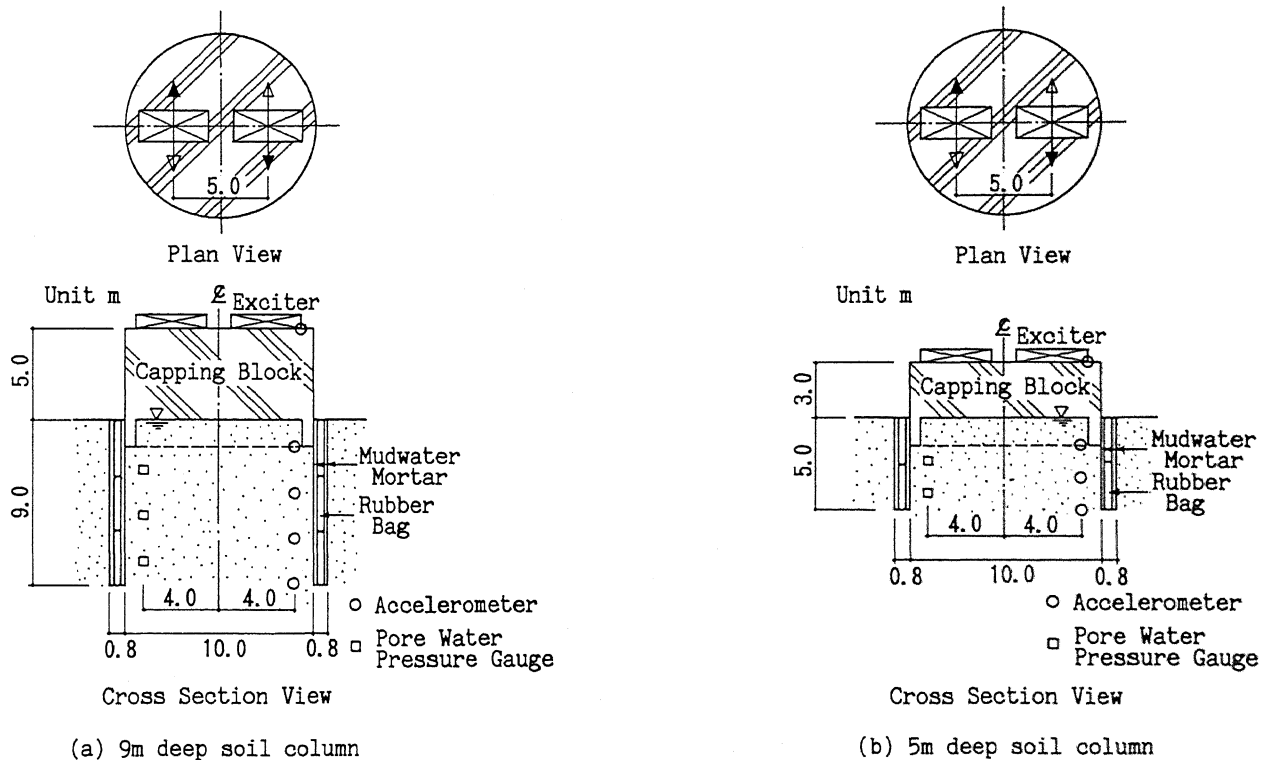


Fig.19 In-situ soil columns for dynamic torsional test

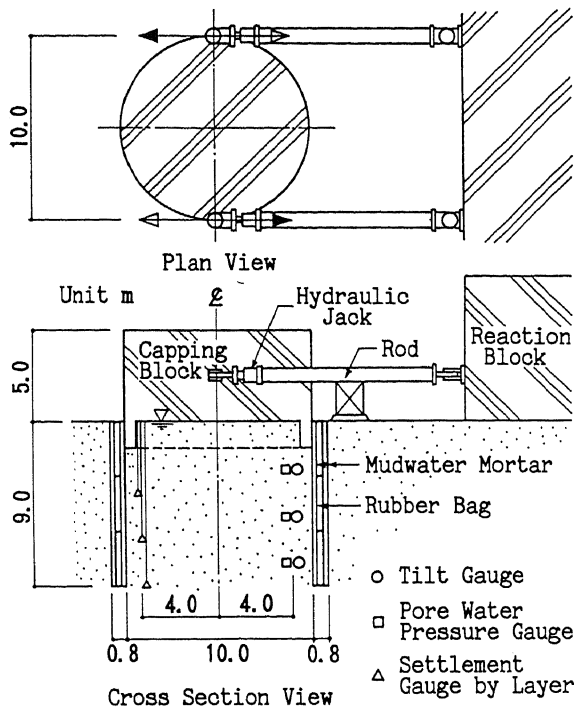


Fig.20 In-situ soil column for static torsional test

Torsional loading method

The dynamic torsional tests were conducted by applying sinusoidal torsional moments to the 9m and 5m deep soil columns by means of two exciters mounted on top of the capping block operating in opposite phase, as shown in Fig.19. For the 9m deep soil column, the loading moment was increased in 3 steps, 49, 98 and 147kN·m, in order to achieve a small level of shear strain of 10^{-5} . For the 5m deep soil column, the loading moment was increased in 5 steps, 98, 196, 294, 392 and 490kN·m, in order to achieve a medium level of shear strain of 10^{-4} . The loading moment amplitude was constant in each loading step, in which the frequency was changed by an increment of 0.1 Hz.

The static torsional tests were also conducted by applying cyclic torsional moments to the 9m deep soil column by means of two hydraulic jacks installed between the capping block and the reaction block operating in opposite directions, as shown in Fig.20. The loading moment was increased in 6 steps, 8.8, 11.8, 17.7, 23.5, 29.4 and 35.3MN·m, in order to achieve a large level of shear strain of 10^{-3} .

The loading moment amplitude was constant in each loading step, in which 5 cycles of static load with a triangular wave form were applied slowly.

As shown in Table 2, the wide shear strain range from a small level of 10^{-5} to a large level of 10^{-3} was covered in all of the three torsional tests.

Table 2 Strain levels of in-situ soil column test

| No | Level of Shear Strain | Depth of Soil Column | Loading Method |
|----|------------------------|----------------------|----------------|
| 1 | $\sim 10^{-5}$ | 9m | Dynamic |
| 2 | $10^{-5} \sim 10^{-4}$ | 5m | Dynamic |
| 3 | $10^{-4} \sim 10^{-3}$ | 9m | Static |

Measuring instrumentation

In the dynamic torsional tests, the measuring instruments used were accelerometers and pore water pressure gauges, as shown in Fig.19. The accelerometers were installed to measure tangential accelerations of the capping blocks and the soil columns. The pore water pressure gauges were installed to measure the fluctuation of excess pore water pressures in the soil columns.

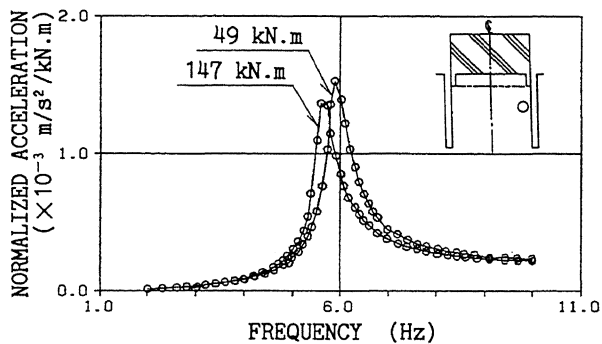
In the static torsional tests, the measuring instruments used were tilt gauges, pore water pressure gauges and settlement gauges, as shown in Fig.20. The tilt gauges were installed to measure tangential shear strains of the soil column. The pore water pressure gauges were installed to measure the fluctuation of excess pore water pressures in the soil column. The settlement gauges were installed to measure the vertical deformations of the soil column.

TORSIONAL TEST RESULTS ON IN-SITU SOIL COLUMNS

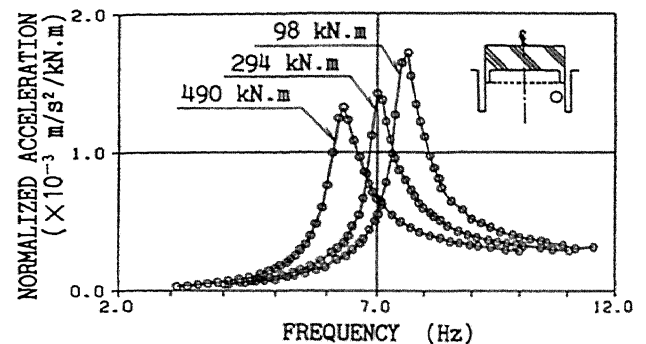
Dynamic torsional tests

Fig.21 shows the acceleration resonance curves of the soil columns and Fig.22 shows the relations between the shear strain of the soil column at the resonance frequency and the torsional loading moment. The shear strain was calculated from the relative displacement obtained by integrating the acceleration twice. The relative displacement was divided by the vertical distance between the accelerometers. As shown in Fig.22, the intended levels of shear strain of 10^{-5} and 10^{-4} are achieved respectively for the 9m and 5m deep soil columns.

As shown in Fig.21, the resonance frequency and the amplification ratio of the acceleration of the 9m deep soil column decrease slightly as the torsional loading moment increases, and those of the 5m deep soil column decrease even more in comparison with the results of the 9m deep soil column. It indicates that the stiffness of the soil columns was reduced and the damping increased as the shear strain increased in the soil columns. Regarding the pore water pressure, for the 9m deep soil column the excess pore water pressure fluctuated at the same frequency as the torsional loading moment, and for the 5m deep soil column the excess pore water pressure fluctuated at twice the frequency of the torsional loading moment due to the effect of dilatancy. However, for both the 9m and 5m deep soil columns accumulation of the excess pore water pressure was not observed in the shear strain range smaller than 10^{-4} .

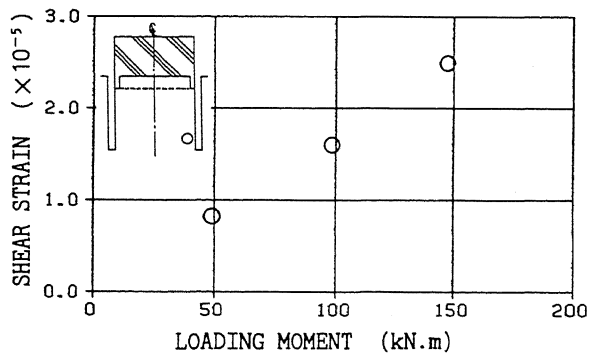


(a) 9m deep soil column

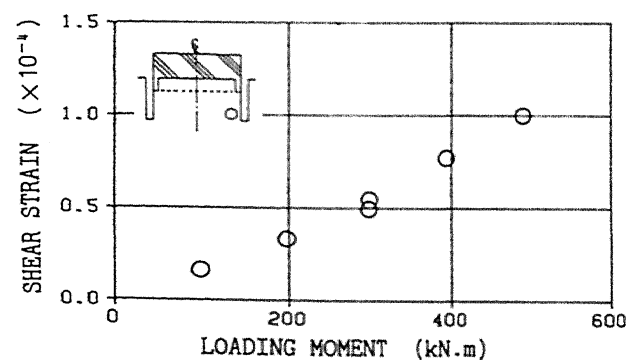


(b) 5m deep soil column

Fig.21 Acceleration resonance curves in dynamic torsional test of in-situ soil columns



(a) 9m deep soil column



(b) 5m deep soil column

Fig.22 Relations between shear strain at resonance frequency and torsional loading moment in dynamic torsional test of in-situ soil columns

Static torsional tests

Fig.23 shows the shear strain-torsional loading moment curves of the soil column in the loading steps 8.8, 23.5 and 35.3 MN·m. Fig.24 shows the relations between the shear strain of the soil column and the torsional loading moment at the final cycle in each test. In Fig.24, one half of a double amplitude of the shear strain at the final cycles is indicated.

As shown in Fig.23, the intended level of shear strain of 10^{-3} is achieved in the tests. The shear

strain-torsional loading moment curve shows a spindle shaped pattern inherent in soil material and it also draws stable hysteresis loops in the large level of shear strain of 10^{-3} . As shown in Fig.24, the amplification ratio of the shear strain of the soil column increases largely as the torsional loading moment increases. It indicates that the stiffness of the soil column was reduced significantly as the shear strain increased to the level of 10^{-3} .

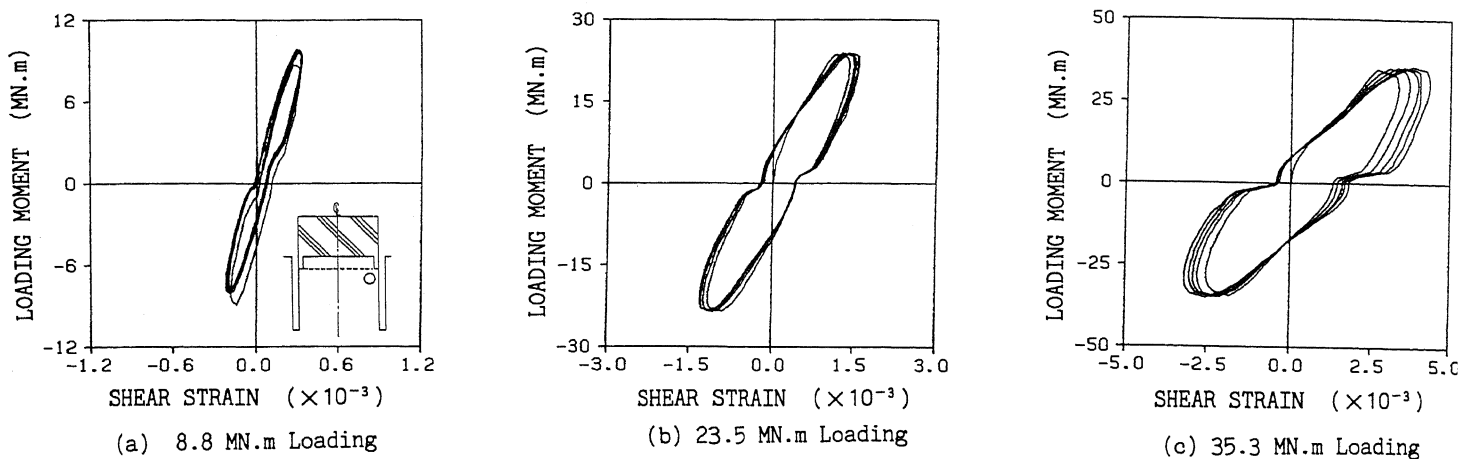


Fig.23 Shear strain-torsional loading moment curves in static torsional test of in-situ soil column

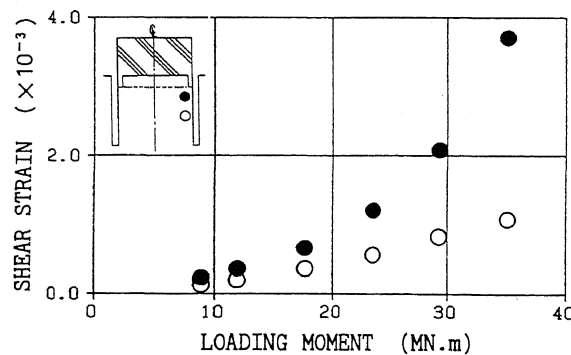


Fig.24 Relations between shear strain and torsional loading moment in static torsional test of in-situ soil column

Fig.25 shows the vertical deformation-torsional loading moment curves in the loading steps 8.8, 23.5 and 35.3 MN·m and Fig.26 shows the relations between the residual vertical deformation of the soil column and the torsional loading moment in each test.

As shown in Fig.25, the vertical deformation is upward in expansion during loading and downward in compression during unloading due to the dilatancy inherent in dense sand or gravel material. Then, with increasing number of loading cycle the vertical deformation continues to accumulate in the direction of compression.

As shown in Fig.26, when the torsional loading moment becomes larger than 23.5 MN·m the residual vertical deformation increases largely, and accumulation of the residual vertical deformation became noticeable in the shear strain range larger than 10^{-3} .

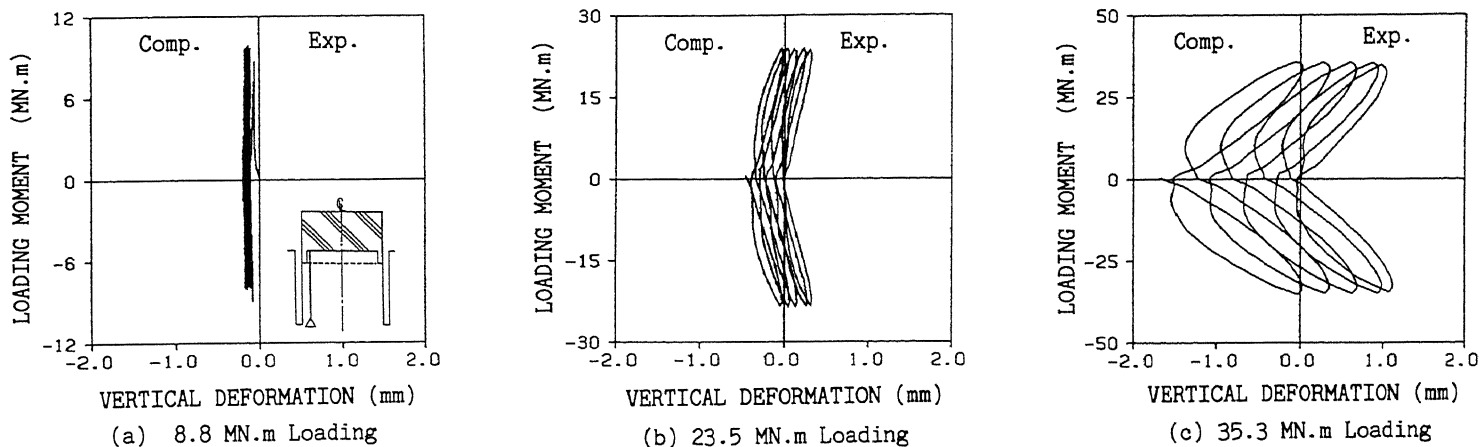


Fig.25 Vertical deformation-torsional loading moment curves in static torsional test of in-situ soil column

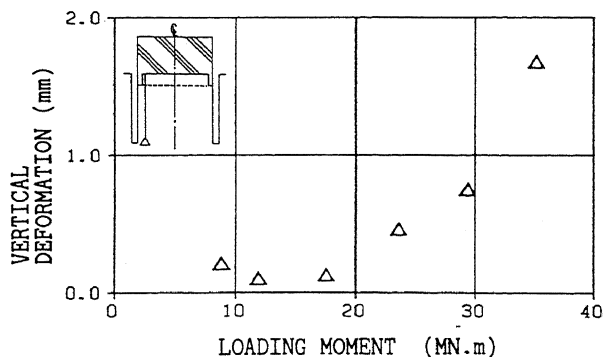


Fig.26 Relations between residual vertical deformation and torsional loading moment in static torsional test of in-situ soil column

Regarding the pore water pressure, the excess pore water pressure fluctuated at twice the frequency of the torsional loading moment due to the effect of dilatancy as shown in Fig.27. However, the excess pore water pressure did not accumulate, because halts of operation of the hydraulic jacks for a while at zero loading caused dissipation of the excess pore water pressure. Instead, accumulation of the vertical deformation was observed.

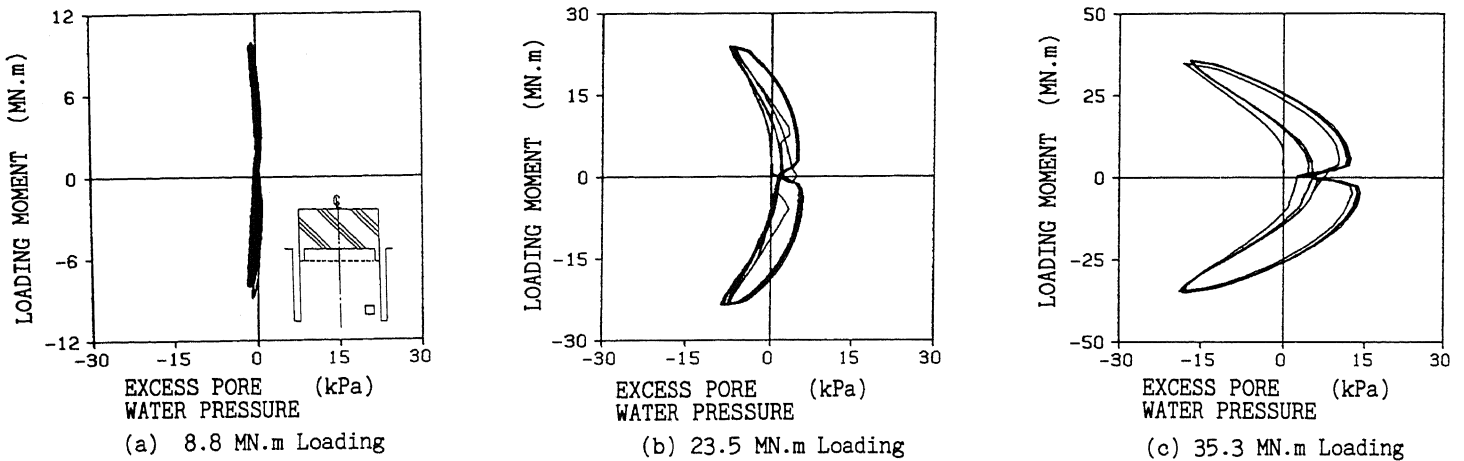


Fig.27 Excess pore water pressure-torsional loading moment curves in static torsional tests of in-situ soil column

SOIL PROPERTIES BY LABORATORY TESTS AND IN-SITU SOIL COLUMN TESTS

Back analysis of in-situ soil column test results

The back analyses were conducted using the measured data of the in-situ soil column tests in order to clarify the cyclic deformation characteristics of the gravelly soil layer quantitatively. In the dynamic torsional tests, the soil columns were represented by one-stick lumped mass models for torsional mode, as shown in Fig.28. In the back analyses, complex torsional spring constants in the lumped mass models were back-calculated using the torsional loading moment and the measured accelerations as input data in each loading step. Then, shear moduli and damping ratios of the soil columns at each shear strain were obtained using the formula of the torsional spring constant of a cylinder.

In the static torsional tests, the soil column was represented by a one-stick discrete model for torsional mode, as shown in Fig.28. In the back analyses, shear stresses in the discrete model were back-calculated using the torsional loading moment and the measured maximum shear strains as input data in each loading step. Then, equivalent shear moduli and equivalent damping ratios of the soil column at each shear strain were obtained using hysteresis loops which consisted of the calculated shear stress and the measured shear strain.

The shear modulus at small shear strain ($=10^{-5}$), G_0 , the shear strain at which the shear modulus was reduced to one half, $\gamma_{0.5}$, and the strain dependency of shear modulus and damping ratio were obtained from the back analysis results of the dynamic and static torsional tests.

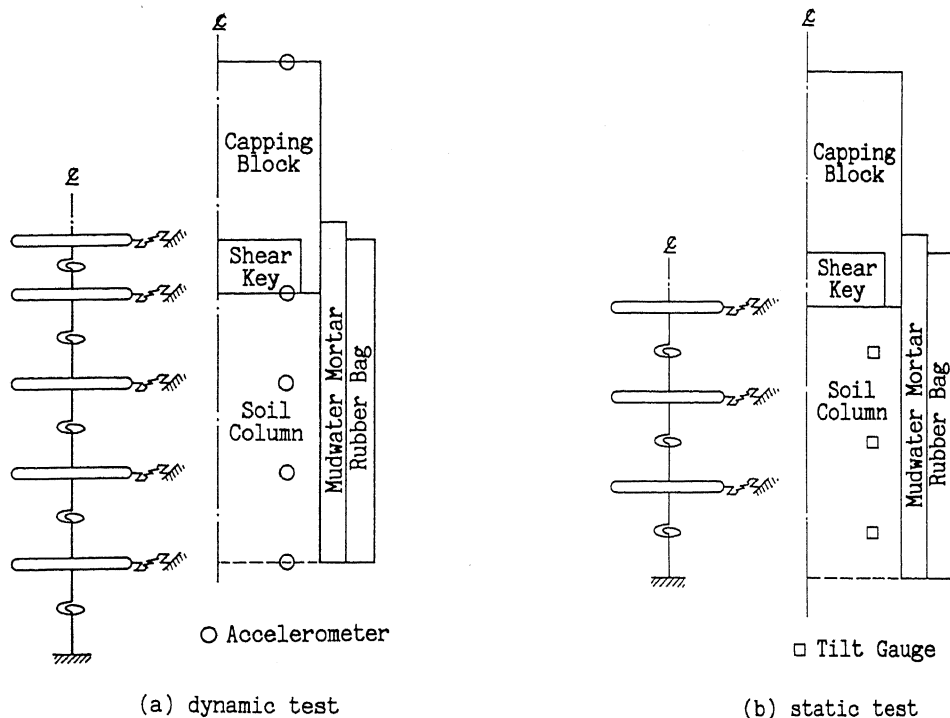


Fig.28 Models of back analysis for in-situ soil column test

Comparison of soil properties

The cyclic deformation characteristics of the gravelly soil layer obtained from the in-situ soil column tests are compared with those obtained from the laboratory tests and the other field tests.

(1) Shear modulus at minute strain

Shear modulus at minute strain, G_0 , obtained from three different methods; laboratory test, back analysis on the in-situ soil column test results and in-situ elastic wave test are plotted in Fig.29 with the confining stress, $\sigma' c'$, on both logarithmic coordinates. Followings can be pointed out.

1) Though the G_0 values determined from the back analysis on the in-situ soil column test results are more scattered compared with the G_0 obtained from the laboratory tests, it can be seen that the G_0 obtained from the in-situ soil column tests also has a dependency on the confining stress.

2) Among three methods for determination of G_0 for the same confining stress, the in-situ elastic wave method gives the largest value of

G_0 , the laboratory test results show the smallest value, and the in-situ soil column tests provide a value between these two. Generally speaking, the difference of the G_0 obtained from the in-situ elastic wave test, the laboratory test on undisturbed samples and the in-situ soil column test is considered due to the following reasons.

- ① In the in-situ elastic wave test, the shortest travelling time through the target soil layer is measured for determination of shear wave velocity, V_s . It can be considered that the in-situ elastic wave test presents the largest value of V_s and G_0 .
- ② The strain level corresponding to the G_0 measured in the in-situ elastic wave test is only known qualitatively as a very small value, may be smaller than 10^{-6} . Unlike the in-situ elastic wave test, in the laboratory tests on undisturbed samples and the in-situ soil column tests, the exact strain level is known and it is usually larger than 10^{-5} . In most cases, the strain level induced in the soil sample is larger than that in the in-situ elastic wave test.
- ③ In order to perform the laboratory tests on undisturbed samples, confining stress must be estimated and applied on the samples before cyclic loading. It is widely known and is also clearly shown in the present study that

Go depends on effective mean principal stress. This means that the correct estimation of Go of in-situ soils requires correct estimation of effective mean principal stress. Then, it indicates that the in-situ lateral stress of gravelly soils is needed to be correctly determined.

However, unfortunately, there is no reliable method developed for determination of in-situ lateral stress of cohesionless soil at present. As a result, the measurement of Go on undisturbed samples is essentially not good enough until a reliable method for determination of in-situ lateral stress is developed.

④ The shear modulus and damping ratio are significantly affected by the method for measuring the deformation of soil sample, especially harder soil sample such as dense sand and gravel, during cyclic loading. According to the data presented by Tatsuoka et al (1992), even though the non-contact pressure gauge is used for measuring the axial displacement, there will be fairly large overestimation of axial displacement

due to an unfavorable clearance between a displacement transducer and a test specimen and bedding error.

More efforts are required to decrease the influence due to these factors on the shear modulus at minute strain.

(2) Strain dependency of shear modulus and damping ratio

Fig.30 shows $G/G_0 \sim \gamma$, $h \sim \gamma$ relations obtained from the back analysis results of the in-situ soil column tests.

Fig.31 shows the relations between the shear strain $\gamma_{0.5}$ at one half of G_0 and the confining stress $\sigma'_{c'}$ obtained both from the laboratory tests and the in-situ soil column tests. As for the laboratory tests, there can be seen almost a straight line relation between $\gamma_{0.5}$ and $\sigma'_{c'}$ on both logarithmic coordinates.

- In-situ soil column test ○ Dynamic load 5m deep
- △ Dynamic load 9m deep
- Soil investigation ◇ Cyclic deformation test ($\gamma_a = 1.824 \sim 2.023$, $e = 0.310 \sim 0.452$)
- ◆ In-situ elastic wave test

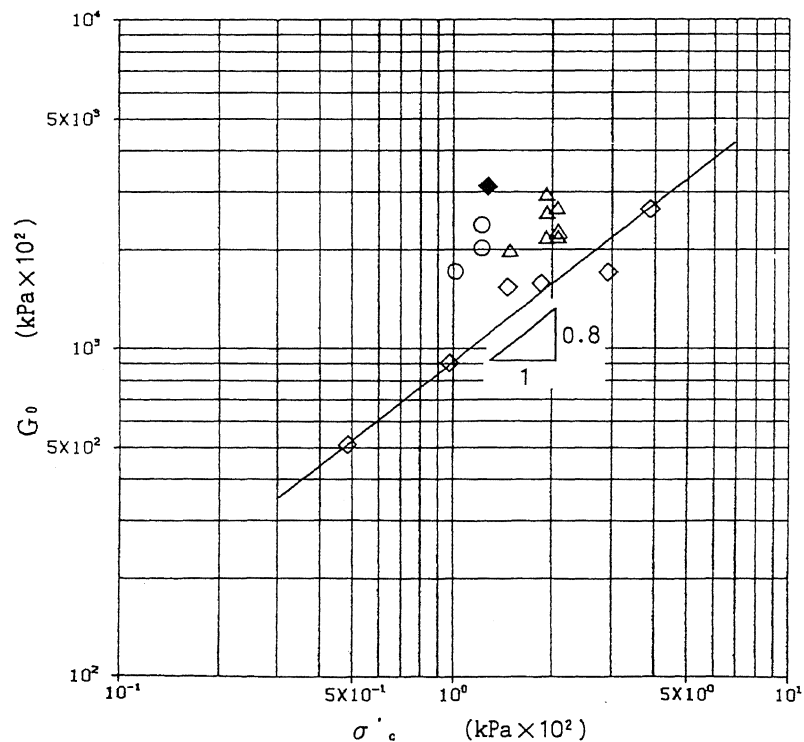


Fig.29 Relations between G_0 and $\sigma'_{c'}$ obtained from in-situ soil column test, laboratory test and field test

The slope of the line is about 0.1, which is much smaller than the value of 0.6 for sand as reported by Ishihara(1982). The low dependency on $\sigma c'$ of $\gamma 0.5$ of undisturbed gravelly soil compared with sand is corresponding to its higher dependency on $\sigma c'$ of G_0 shown in the equation (2) as described below. The $\gamma 0.5$ in Hardin-Drnevich model is defined by the equation(3). The strength, τf , is related to $\sigma c'$ in the form as shown in the equation (4) for cohesionless soil . Submitting the equation (2) and equation (4) into the equation (3), the equation (5) can be derived. The equation (5) indicates the possibility of low dependency on $\sigma c'$ of $\gamma 0.5$, and this expectation is in good agreement with the laboratory test results between G_0 and $\sigma c'$ as described before.

$$G_0 = A(\sigma c')^{0.8} \quad (2)$$

$$\gamma 0.5 = \tau f / G_0 \quad (3)$$

$$\tau f = \sigma c' \tan \phi \quad (4)$$

$$\gamma 0.5 = (\sigma c')^{0.2} \tan \phi / A \quad (5)$$

where,

A ; constant, ϕ ; internal friction angle

On the other hand, $\gamma 0.5$ obtained from the in-situ soil column tests has a much higher dependency on $\sigma c'$ as shown in Fig.31 than that obtained from the laboratory tests. This higher dependency

on $\sigma c'$ of $\gamma 0.5$ obtained from the in-situ soil column tests is thought to be affected by the decrease of shear modulus due to the disturbance in the soil column during cyclic loading, especially in the low confining stress portion of the soil column.

Fig.32 shows $G/G_0 \sim \gamma / \gamma 0.5$ relations and $h \sim \gamma / \gamma 0.5$ relations obtained both from the laboratory tests and the in-situ soil column tests. There can be seen a good agreement of the $G/G_0 \sim \gamma / \gamma 0.5$ relations obtained from the laboratory tests and the in-situ soil column tests. The $h \sim \gamma / \gamma 0.5$ relations obtained from the in-situ soil column tests are scattered to some extent compared with those obtained from the laboratory tests. But the similar tendency that the damping ratio increases from about 2% to 15% with increasing shear strain can be seen. Based on the comparisons described above, it was suggested that the $G/G_0 \sim \gamma / \gamma 0.5$ relations and the $h \sim \gamma / \gamma 0.5$ relations can be reliably determined from the laboratory tests on undisturbed samples, so we need not always perform the large in-situ soil column test, which is costly and time consuming.

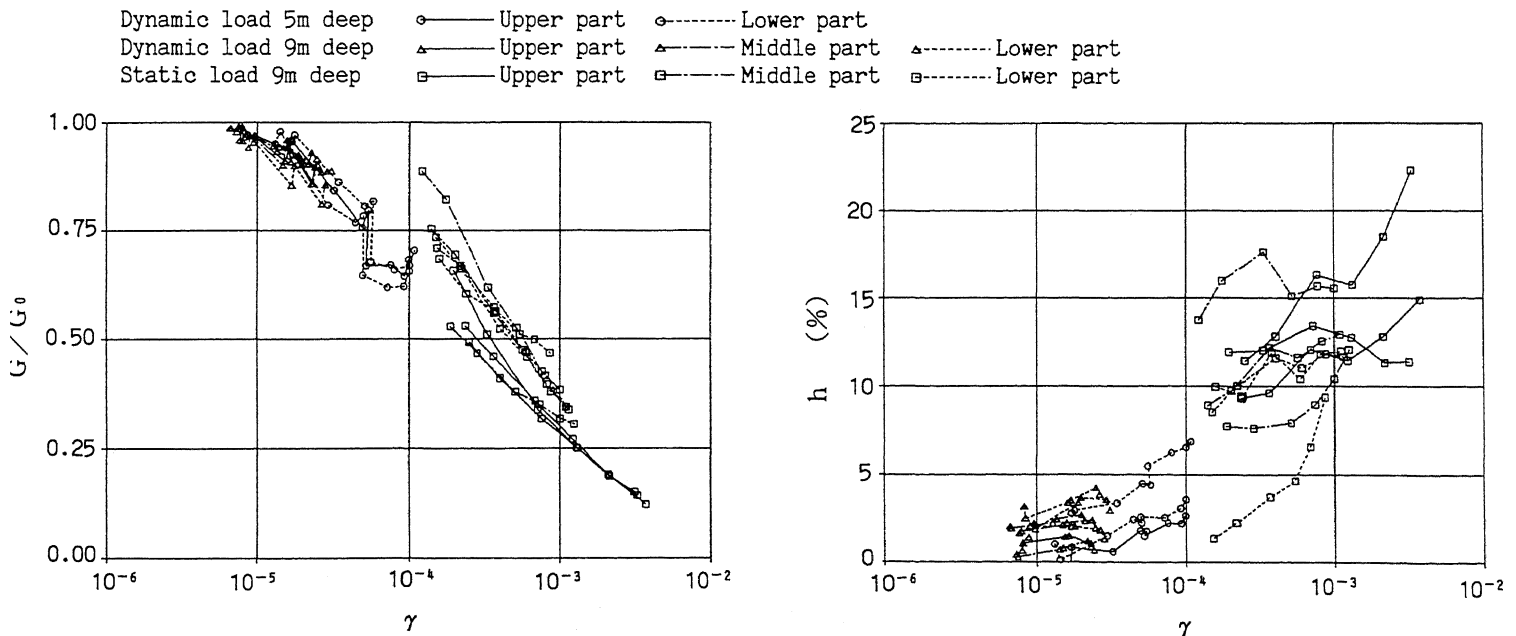


Fig.30 $G/G_0 \sim \gamma$, $h \sim \gamma$ relations obtained from in-situ soil column test

In-situ soil column test ○ Dynamic load 5m deep
 △ Static load 9m deep
 Soil investigation ◆ Cyclic deformation test ($\gamma_d = 1.824 \sim 2.023$, $e = 0.310 \sim 0.452$)

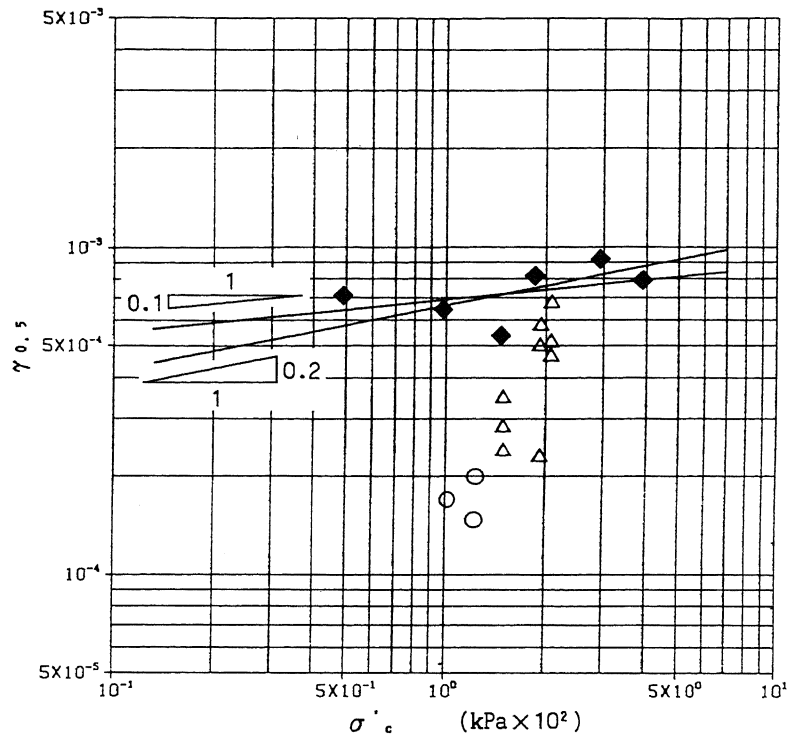


Fig.31 Relations between $\gamma_{0.5}$ and $\sigma' c$ obtained from in-situ soil column test and laboratory test

In-situ soil column test ○ Dynamic load 5m deep
 △ Dynamic load 9m deep
 □ Static load 9m deep
 Soil investigation ◆ Cyclic deformation test ($\gamma_d = 1.824 \sim 2.023$, $e = 0.310 \sim 0.452$)

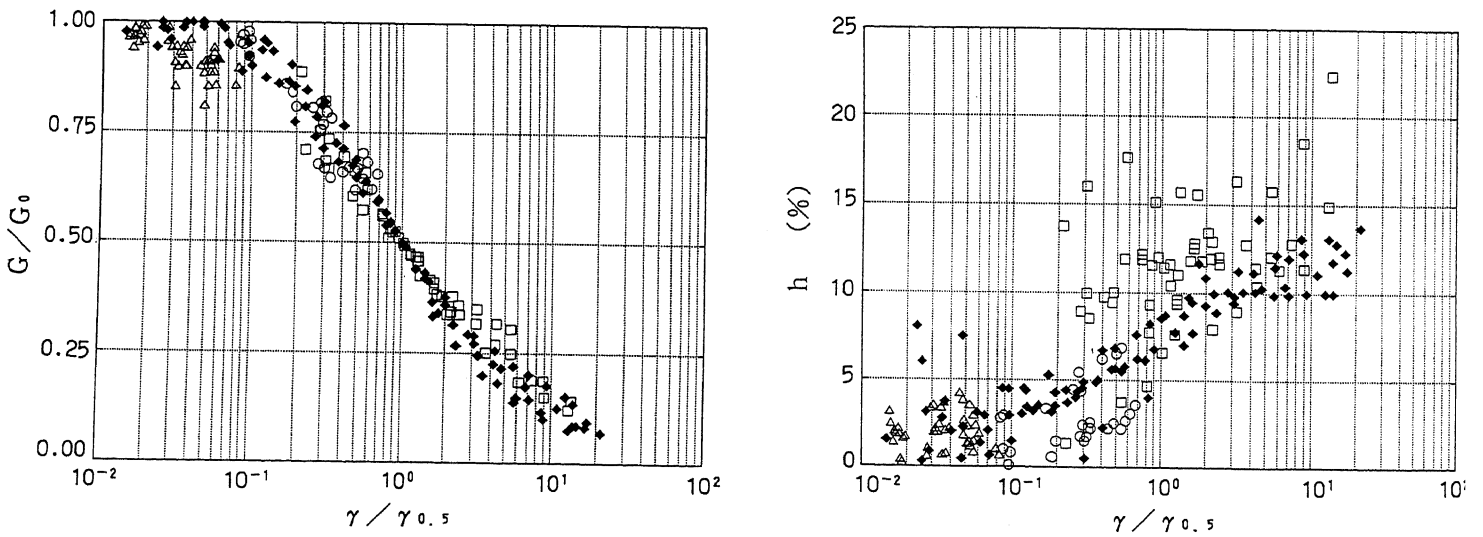


Fig.32 $G/G_0 \sim \gamma / \gamma_{0.5}$, $h \sim \gamma / \gamma_{0.5}$ relations obtained from in-situ soil column test and laboratory test

CONCLUSIONS

The following conclusions are obtained through laboratory tests on high quality undisturbed samples of gravelly soil which were obtained from a depth of 11m below the ground surface by the in-situ freezing method using a large scale triaxial test apparatus.

- (1) There is a significant difference of undrained cyclic shear strength between undisturbed and reconstituted specimen. For example, the stress ratio required to cause double amplitude shear strain of 2.5% in 20 cycles of stress application for the undisturbed specimens is about twice the value of the reconstituted specimens.
- (2) Compared with the reconstituted specimens, the shear modulus of the undisturbed specimens is about 50% higher in the range of shear strain level smaller than 10^{-2} . The damping ratio of the undisturbed specimen is about 20 to 30% smaller than that of the reconstituted specimens.
- (3) The shear modulus at $\gamma = 10^{-5}$ has a larger dependency on confining stress than that of sand.
- (4) The internal friction angle, ϕ_d , is ranged between 36 and 37 degrees, which is not so large as was expected for their high SPT N-values. On the other hand, cohesion values ranging from 24.5 to 66.6kPa was observed.

From the results of the cyclic torsional tests on the large-scale soil columns prepared in-situ, the following principal conclusions are obtained.

- (5) It was confirmed that the gravelly soil layer subjected to shear strains in the level between 10^{-5} and 10^{-3} showed a decrease in shear modulus and an increase in damping ratio due to the strain dependency under cyclic loading.
- (6) The excess pore water pressure did not accumulate in the shear strain range smaller than 10^{-4} .
- (7) The volumetric deformation due to the dilatancy accumulated in the direction of compression with increasing number of loading cycle in the shear strain range larger than 10^{-3} .

The shear modulus at minute strain, G_0 , obtained from three different methods ; ① laboratory test, ② back analysis on the in-situ soil column test results and ③ in-situ elastic wave test is discussed. The strain dependency of shear modulus and damping ratio obtained both from the laboratory tests and the in-situ soil column tests is

also discussed. Based on the above discussions, followings are summarized.

- (8) Among three methods for determination of shear modulus at minute strain, G_0 , the in-situ elastic wave method gives the largest value, the laboratory test shows the smallest value, and the in-situ soil column test provides a value between these two.
- (9) The shear strain $\gamma_{0.5}$ at $G/G_0=0.5$ obtained from the laboratory test on undisturbed samples is almost proportional to the 0.1 power of the confining stress, σ_c' . This low dependency on confining stress of $\gamma_{0.5}$ is corresponding to the fact that G_0 depends highly on the σ_c' . It also can be pointed out that the $\gamma_{0.5}$ of undisturbed gravelly soil has much less dependency on σ_c' than that of sand as reported by Ishihara(1982).
- (10) There is no significant difference of the $G/G_0 \sim \gamma / \gamma_{0.5}$ relations and the $h \sim \gamma / \gamma_{0.5}$ relations obtained from the laboratory tests on undisturbed samples and from the in-situ soil column tests.

Based on the test results, the laboratory test using high quality undisturbed samples is a reliable and viable method to determine the strain dependency of cyclic deformation characteristics of in-situ gravelly soils for design purposes.

ACKNOWLEDGEMENTS

This work was carried out by NUPEC as the project sponsored by the Ministry of International Trade and Industry of Japan. This work was reviewed by Committee of Verification Test on Siting Technology for High Seismic Structures of NUPEC. The in-situ frozen sampling was confronted by Tokyo Soil Research Co., Ltd. The authors wish to express their gratitude for the cooperation and valuable suggestions given by every committee member.

REFERENCES

- Hatanaka, M., Sugimoto, M. and Suzuki, Y. (1985): "Liquefaction resistance of two alluvial volcanic soils sampled by in-situ freezing", Soils and Foundations, Vol.25, No.3, pp. 49-63.

- Hatanaka, M., Suzuki, Y., Kawasaki, T. and Endo, M. (1988): "Cyclic undrained shear properties of high quality undisturbed Tokyo gravel", *Soils and Foundations*, Vol.2, No.4, pp.57-68.
- Ishihara, K.(1982) : " Evaluation of soil properties for use in earthquake response analysis", *International Symposium on Numerical Models in Geomechanics*, Zurich, pp.237-259.
- Suzuki, Y., Hatanaka, M., Konno, T., Ishihara, K. and Akino, K.(1992) : " Engineering properties of undisturbed gravel sample", *Proc.10th World Conference on Earthquake Engineering*, Madrid, Vol.3, pp.1281-1286.
- Tateishi, A., Takayanagi, T., Ishihara, K., Hayashi, M., Iizuka, S. and Suzuki, S. (1992) : " Torsional tests on large in-situ soil columns", *Proc.10th World Conference on Earthquake Engineering*, Madrid, Vol.3, pp.1305-1310.
- Tatsuoka, F. and Shibuya, S. (1992) : "Deformation characteristics of soils and rocks from field and laboratory tests", *Report of the Institute of Industrial Science, University of Tokyo*, Vol.37, No.1.
- Watabe, M., Hayashi, M., Ishihara, K., Akino, K., Iizuka, S., Ukita, T., Yamazaki, T., Konno, T., Suzuki, S., Kitazawa, K., Suzuki, Y., Matsuda, T., Mori, K. and Nagai, K.(1991) : " Large scale field tests on quaternary sand and gravel deposits for seismic siting technology ", *Proc. 2nd International Conference on Recent Advances in Geotechnical Earthquake Engineering and Soil Dynamics*, St.Louis, pp.271-289.
- Yoshimi, Y., Tokimatsu, K., Kaneko, O. and Makihara, Y. (1984): "Undrained cyclic strength of a dense Niigata sand", *Soils and Foundations*, Vol.24, No.4, pp.131-145.